

**Z' gauge bosons at the Fermilab Tevatron**Marcela Carena,<sup>1</sup> Alejandro Daleo,<sup>1,2</sup> Bogdan A. Dobrescu,<sup>1</sup> and Tim M. P. Tait<sup>1</sup><sup>1</sup>*Theoretical Physics Department, Fermilab, Batavia, Illinois 60510, USA*<sup>2</sup>*Departamento de Física, Universidad Nacional de La Plata, C.C. 67-1900 La Plata, Argentina.*

(Received 6 September 2004; published 12 November 2004)

We study the discovery potential of the Tevatron for a  $Z'$  gauge boson. We introduce a parametrization of the  $Z'$  signal which provides a convenient bridge between collider searches and specific  $Z'$  models. The cross section for  $p\bar{p} \rightarrow Z'X \rightarrow \ell^+\ell^-X$  depends primarily on the  $Z'$  mass and the  $Z'$  decay branching fraction into leptons times the average square coupling to up and down quarks. If the quark and lepton masses are generated as in the standard model, then the  $Z'$  bosons accessible at the Tevatron must couple to fermions proportionally to a linear combination of baryon and lepton numbers in order to avoid the limits on  $Z - Z'$  mixing. More generally, we present several families of U(1) extensions of the standard model that include as special cases many of the  $Z'$  models discussed in the literature. Typically, the CDF and D0 experiments are expected to probe  $Z'$ -fermion couplings down to 0.1 for  $Z'$  masses in the 500–800 GeV range, which in various models would substantially improve the limits set by the LEP experiments.

DOI: 10.1103/PhysRevD.70.093009

PACS numbers: 14.70.Hp, 12.60.Cn

**I. INTRODUCTION**

An important question in particle physics today is whether there are any new gauge bosons beyond the ones associated with the  $SU(3)_C \times SU(2)_W \times U(1)_Y$  gauge group. This question is interesting by itself, given that the selection of the gauge bosons observed so far remains mysterious. Furthermore, new gauge bosons are predicted within many theories beyond the standard model (SM) which have been developed to provide answers to its many open questions.

The simplest way of extending the SM gauge structure is to include a second U(1) group. The associated gauge boson, usually labeled  $Z'$ , is an electrically-neutral spin-1 particle. If the new gauge coupling is not much smaller than unity, then the U(1) group must be spontaneously broken at a scale larger than the electroweak scale in order to account for the nonobservation of the  $Z'$  boson at LEP and run I of the Tevatron. In this article, we study the  $Z'$  discovery potential of the run II of the Tevatron, the highest energy hadron machine operating for the next few years.

The theoretical framework for studying  $Z'$  production at hadron colliders has been developed more than two decades ago [1]. Nevertheless, various pieces of information collected recently have an impact on our attempt of addressing a number of specific questions: What  $Z'$  parameters are relevant for Tevatron searches? What regions of the parameter space are not ruled out by the LEP experiments, and would allow a  $Z'$  discovery at the Tevatron? In case of a discovery, how can one differentiate between the models that may accommodate a  $Z'$  boson?

It is often assumed that the  $Z'$  couplings have certain values motivated by some narrow theoretical assumptions, allowing for the derivation of a  $Z'$  mass bound

[2,3]. The opposite approach of leaving the couplings arbitrary [4] suffers from the existence of too many free parameters. However, a few theoretical constraints are sufficiently generic so that it is reasonable to focus on the region of the parameter space that satisfies them. This observation, used to define the so-called nonexotic  $Z'$  bosons [5], underscores the importance of the  $Z'$  couplings to the SM fermions for collider phenomenology [6], while reducing the set of  $Z'$  parameters.

In this article, we address  $Z'$  models both from a theoretical perspective and with respect to their potential observation at hadron colliders. In Sec. II we present the theoretical framework needed to describe a new neutral gauge boson. We analyze the constraints due to gauge anomaly cancellation and the gauge invariance of the quark and lepton Yukawa couplings, and discuss what new physics would soften these constraints. We identify several interesting families of  $Z'$  models, and then derive the LEP limits. Section III is concerned with  $Z'$  production at hadron colliders, including a survey of theoretical tools to describe  $Z'$  events, and a convenient parametrization of limits from searches that simplifies comparison of experimental results with theoretical models. Section IV summarizes our conclusions.

**II. PARAMETERS DESCRIBING NEW NEUTRAL GAUGE BOSONS**

Any new gauge boson is characterized by a mass and a number of coupling constants. All these parameters appear in the Lagrangian, which is constrained by gauge and Lorentz invariance. In this section we present a theoretical framework that is sufficiently general to account for the parameters that are relevant for  $Z'$  searches at the Tevatron. We discuss the theoretical constraints

within realistic extensions of the SM, and then discuss the LEP limits.

### A. $Z'$ mass and $Z - Z'$ mixing

Consider the SM gauge symmetry extended by one Abelian gauge group,  $SU(3)_C \times SU(2)_W \times U(1)_Y \times U(1)_z$ . The scalar sector responsible for the spontaneous breaking of the gauge symmetry down to  $SU(3)_C \times U(1)_{\text{em}}$  includes at least one Higgs-doublet and an  $SU(2)_W$  singlet,  $\phi$ , with vacuum expectation value (VEV)  $v_\phi$ . As we will explicitly show below, the constraints on the interactions of the  $U(1)_z$  gauge boson with quarks and leptons are relaxed in the presence of two Higgs doublets,  $H_1$  and  $H_2$ , with aligned VEVs  $v_{H_1}$  and  $v_{H_2}$ . To be general, we will concentrate on this case in what follows. The hypercharges of  $H_1$ ,  $H_2$ , and  $\phi$  are given by +1, +1 and 0, respectively, so that electric charge is conserved.

In a basis where the three electrically-neutral gauge bosons,  $W^{3\mu}$ ,  $B_Y^\mu$  and  $B_z^\mu$ , have diagonal kinetic terms, their mass terms are given by:

$$\begin{aligned} & \frac{v_{H_1}^2}{8} (gW^{3\mu} - g_Y B_Y^\mu - z_{H_1} g_z B_z^\mu)^2 + \frac{v_{H_2}^2}{8} (gW^{3\mu} - g_Y B_Y^\mu \\ & - z_{H_2} g_z B_z^\mu)^2 + \frac{v_\phi^2}{8} (z_\phi g_z B_z^\mu)^2, \end{aligned} \quad (2.1)$$

where  $g$ ,  $g_Y$ ,  $g_z$  are the  $SU(2)_W \times U(1)_Y \times U(1)_z$  gauge couplings, and the weak mixing angle is given as usual by  $\tan\theta_w = g_Y/g$ . The diagonalization of these mass terms yields the three physical states, the photon (labeled by  $A^\mu$ ), the observed  $Z$  boson, and the hypothetical  $Z'$  boson:

$$\begin{aligned} A_\mu &= W^{3\mu} \sin\theta_w + B_Y^\mu \cos\theta_w, \\ Z_\mu &= W^{3\mu} \cos\theta_w - B_Y^\mu \sin\theta_w + \epsilon B_z^\mu, \\ Z'_\mu &= B_z^\mu - \epsilon (W^{3\mu} \cos\theta_w - B_Y^\mu \sin\theta_w). \end{aligned} \quad (2.2)$$

To obtain this result we have ignored terms of order  $\epsilon^2$ , where  $\epsilon$  is the mixing angle between the SM  $Z$  boson and  $B_z^\mu$ ,

$$\epsilon = \frac{\delta M_{ZZ'}^2}{M_{Z'}^2 - M_Z^2}. \quad (2.3)$$

The mass-squared parameters introduced here are related to the VEVs by

$$\begin{aligned} M_Z^2 &= \frac{g^2}{4\cos^2\theta_w} (v_{H_1}^2 + v_{H_2}^2) [1 + O(\epsilon^2)], \\ M_{Z'}^2 &= \frac{g_z^2}{4} (z_{H_1}^2 v_{H_1}^2 + z_{H_2}^2 v_{H_2}^2 + z_\phi^2 v_\phi^2) [1 + O(\epsilon^2)], \\ \delta M_{ZZ'}^2 &= -\frac{gg_z}{4\cos\theta_w} (z_{H_1} v_{H_1}^2 + z_{H_2} v_{H_2}^2). \end{aligned} \quad (2.4)$$

$M_Z$  and  $M_{Z'}$  are the physical masses of the neutral gauge bosons up to corrections of order  $\epsilon^2$ .

A  $Z'$  boson which mixes with the SM  $Z$  distorts its properties, such as couplings to fermions and mass relative to electroweak inputs. Precision measurements of observables, mostly on the  $Z$  pole at LEP I and Stanford Linear Accelerator, have verified the SM  $Z$  properties at or below the per mil level<sup>1</sup> [7], imposing a severe upper bound [10] on the mixing angle between the  $Z$  and  $Z'$ :  $|\epsilon| \lesssim 10^{-3}$ . Therefore, it is justified to treat the mixing as a perturbation as was done above.

From Eqs. (2.3) and (2.4) it follows that the mixing angle is given by

$$|\epsilon| \approx \frac{g_z}{g} \left( \frac{\cos\theta_w}{M_{Z'}/M_Z - 1} \right) \frac{|z_{H_1} + z_{H_2} \tan^2\beta|}{1 + \tan^2\beta} \quad (2.5)$$

where  $\tan\beta = v_{H_2}/v_{H_1}$ . At least one of  $v_{H_1}$  or  $v_{H_2}$  has to be of the order of the electroweak scale (to generate  $M_W$ ,  $M_Z$  and  $m_t$  appropriately), so without loss of generality we can set  $v_{H_2} \sim O(246)$  GeV. Therefore,  $\tan\beta \gtrsim O(1)$ .

Normalizing the largest quark  $U(1)_z$  charges to be of order unity, the  $Z'$  production at the Tevatron is sizable only if the gauge coupling  $g_z$  is not much smaller than unity. The mass range typically interesting at the Tevatron is roughly  $0.2 \text{ TeV} < M_{Z'} < 0.7 \text{ TeV}$ . Based on these considerations we find that the order of magnitude of the mixing angle is given by  $\epsilon \sim (z_{H_1} \cot^2\beta + z_{H_2}) M_Z^2/M_{Z'}^2$ . The constraint  $|\epsilon| \lesssim 10^{-3}$  implies  $z_{H_1} \cot^2\beta + z_{H_2} \ll 1$ . Although  $\tan^2\beta$  could be close to  $-z_{H_1}/z_{H_2}$ , this would be a fine-tuning, because the value of  $\tan\beta$  is set by the Higgs masses and self-interactions, and has no reason to be related to the ratio of Higgs charges. Therefore, in the absence of fine-tuning, a  $Z'$  accessible at the Tevatron requires  $|z_{H_2}| \ll 1$  and either  $|z_{H_1}| \ll 1$  or  $\tan\beta \gg 1$ . It is usually expected that the charges of various fields are either all of the same order or vanish. Although exceptions exist, such as extra dimensional models with brane kinetic terms [11] on the Higgs brane, which motivate much a smaller effective charge for the Higgs than for the (bulk) fermions, we restrict attention here to the following two cases:

$$z_{H_2} = 0 \quad \text{and} \quad z_{H_1} = 0 \quad (2.6)$$

<sup>1</sup>The notable exception is  $\sin^2\theta_w$  from hadronic  $Z$  decays, which deviates at the few  $\sigma$  level [7], and plays an interesting role in the fit to the SM Higgs mass [8]. These deviations have been argued as evidence for the existence of a  $Z'$  with non-universal interactions [9]; we shall not pursue this line of reasoning here.

or

$$z_{H_2} = 0 \quad \text{and} \quad \tan\beta \gtrsim 10. \quad (2.7)$$

### B. Couplings to fermions

The renormalizable interactions of the  $Z'$  boson with the SM fermions are described by the following terms in the Lagrangian density:

$$\sum_f z_f g_z Z'_\mu \bar{f} \gamma^\mu f, \quad (2.8)$$

where  $f = e_R^j, l_L^j, u_R^j, d_R^j, q_L^j$  are the usual lepton and quark fields in the weak eigenstate basis;  $l_L^j = (\nu_L^j, e_L^j)$  and  $q_L^j = (u_L^j, d_L^j)$  are the  $SU(2)_W$  doublet fermions. The index  $j$  labels the three fermion generations. Altogether there are 15 fermion charges,  $z_f$ .

The observed quark and lepton masses and mixings restrict these fermion charges, so that certain gauge and Lorentz invariant terms can appear in the Lagrangian. In the SM, the terms responsible for the charged fermion masses are

$$\lambda_{jk}^d \bar{q}_L^j d_R^k H + \lambda_{jk}^u \bar{q}_L^j u_R^k i\sigma_2 H^\dagger + \lambda_{jk}^e \bar{l}_L^j e_R^k H + \text{h.c.}, \quad (2.9)$$

where  $j, k = 1, 2, 3$  label the fermion generations, and  $\lambda_{jk}^d, \lambda_{jk}^u, \lambda_{jk}^e$  are Yukawa couplings. In the two-Higgs-doublet model described above, the Higgs-doublet  $H$  is replaced by linear combinations of  $H_1$  and  $H_2$ .

As discussed in Sec. II A, the  $Z'$  bosons relevant for Tevatron searches have small mixing with the  $Z$  boson, which effectively implies that any Higgs-doublet with a VEV of order the electroweak scale is neutral under the  $U(1)_z$  symmetry. In particular, if only one Higgs-doublet is present, then its  $U(1)_z$  charge would have to vanish. Given that the total charge of the quark mass terms shown in Eq. (2.9) has to be zero, the quark masses and Cabibbo-Kobayashi-Maskawa quark-mixing matrix (CKM) elements may then be accommodated only if the quarks have generation-independent  $U(1)_z$  charges, and  $z_u = z_d = z_q$ , where  $z_u$  and  $z_d$  are the right-handed up- and down-type quark charges, and  $z_q$  is the left-handed quark doublet charge. One may relax this condition in the two-Higgs-doublet model if, for example,  $H_2$  couples to the up-type quarks, while  $H_1$  couples to the down-type quarks, has nonzero charge, and  $\tan\beta$  is large. In that case  $z_d$  may be different from  $z_u$  and  $z_q$ , but one still needs to impose

$$z_u = z_q, \quad (2.10)$$

so that the large top-quark mass may be generated.

We emphasize that we have derived this strong conclusion based on reasonable but not infallible arguments. One loophole is that some of the terms in Eq. (2.9) may be replaced by higher-dimensional operators such as

$\bar{q}_L^j d_R^k H (\phi/M_{\text{heavy}})^p$ , where  $p$  is an integer and  $M_{\text{heavy}}$  is the mass scale where this dimension- $(4+p)$  operator is generated. Since the weak-singlet scalar  $\phi$  has a nonzero charge under  $U(1)_z$ , the relations between the various quark charges may be changed. The higher-dimensional operators may be induced in a renormalizable quantum field theory by the exchange of heavy fermions that have Yukawa couplings to both the Higgs doublets and  $\phi$ . Another loophole is that both Higgs doublets may be charged under  $U(1)_z$  if there is a fine-tuning as discussed in Sec. II A, so that the restrictions on quark charges would be again modified. Based on these considerations, we will study in some detail the implications of Eq. (2.10), but we will also consider departures from it.

We point out that generation dependent quark charges lead to flavor-changing couplings of the  $Z'$  in the mass eigenstate basis, where the fermion mass matrices are diagonal. Various experimental constraints from flavor-changing neutral current processes impose severe constraints on such flavor-changing  $Z'$  couplings, unless  $M_{Z'}$  is so large that the effects of such a  $Z'$  would be beyond the reach of even the LHC. To avoid these complications we will avoid generation dependent quark charges in this paper. In practice this does not restrict significantly the generality of our results because the Tevatron is typically not very sensitive to  $Z'$  decaying into quarks, and the production cross section depends only on an average quark charge. Therefore, altogether there are three quark charges relevant in what follows:  $z_u, z_d, z_q$ .

The masses of the electrically-charged leptons can be induced by the last term shown in Eq. (2.9) even if the lepton  $z$ -charges are generation dependent. Moreover, no flavor-changing neutral currents are induced in the lepton sector by  $Z'$  exchange. The lepton mass terms impose, though, a relation between the left- and right-handed lepton  $z$ -charges:  $z_{l_j} = z_{e_j}$ ,  $j = 1, 2, 3$ , or  $z_{l_j} - z_{e_j} = z_{H_1}$  in the two-Higgs-doublet model with large  $\tan\beta$ . As in the case of the quarks, we allow for deviations from these equalities motivated by lepton mass generation via higher-dimensional operators. Thus, all six lepton charges,  $z_{l_j}, z_{e_j}$ ,  $j = 1, 2, 3$  could be relevant for Tevatron studies.

Additional constraints arise due to the requirement of generating neutrino masses and mixings. The terms in the Lagrangian responsible for these are given by

$$\frac{c_{jk}}{M_\nu} \bar{l}_L^j l_L^k H^\dagger i\sigma_2 H + \lambda_{jk}^\nu \bar{l}_L^j i\sigma_2 \nu_R^{k'} H^\dagger + m_{j'k'}^\nu \bar{\nu}_R^{j'} \nu_R^{k'} + \text{h.c.}, \quad (2.11)$$

where we have included right-handed neutrinos,  $\nu_R^{j'}$ , which are singlets under the SM gauge group. If these are not present, then the last two terms in the above equation vanish. If there are  $n$  right-handed neutrino flavors, then  $j', k' = 1, \dots, n$ . For  $n \geq 2$  all dimensionless

coefficients  $c_{jk}$  of the above lepton-number-violating terms may vanish. The other parameters appearing in Eq. (2.11) are as follows:  $M_\nu$  is the mass scale where the lepton-number-violating terms are generated,  $m_{jk}^\nu$  are right-handed neutrino Majorana masses,  $\lambda_{jk}^\nu$  are some Yukawa couplings.

The requirement that the three active neutrinos mix, so that the observed neutrino oscillations can be accommodated, implies that the lepton charges are generation independent. However, as in the case of quarks, the terms in Eq. (2.11) may be replaced by higher-dimensional operators involving powers of  $\phi/M_{\text{heavy}}$ . Furthermore, the tiny neutrino masses make the existence of such higher-dimensional operators an attractive possibility [5]. If several  $\phi$  scalars carry different  $U(1)_z$  charges, one could avoid almost entirely the constraints from neutrino mixing on lepton charges.

The six lepton charges determine the leading decay width of the  $Z'$  into the corresponding leptons:

$$\begin{aligned}\Gamma(Z' \rightarrow e_j^+ e_j^-) &\approx (z_{l_j}^2 + z_{e_j}^2) \frac{g_z^2}{24\pi} M_{Z'}, \\ \Gamma(Z' \rightarrow \nu_L \bar{\nu}_L) &\approx (z_{l_1}^2 + z_{l_2}^2 + z_{l_3}^2) \frac{g_z^2}{24\pi} M_{Z'},\end{aligned}\quad (2.12)$$

where  $e_j = \{e, \mu, \tau\}$  for  $j = 1, 2, 3$ . Similarly, the quarks charges determine the following decay widths of the  $Z'$ :

$$\begin{aligned}\Gamma(Z' \rightarrow \text{jets}) &\approx (2z_q^2 + z_u^2 + z_d^2) \frac{g_z^2}{4\pi} M_{Z'} \left(1 + \frac{\alpha_s}{\pi}\right), \\ \Gamma(Z' \rightarrow b\bar{b}) &\approx (z_q^2 + z_d^2) \frac{g_z^2}{8\pi} M_{Z'} \left(1 + \frac{\alpha_s}{\pi}\right), \\ \Gamma(Z' \rightarrow t\bar{t}) &\approx (z_q^2 + z_u^2) \frac{g_z^2}{8\pi} M_{Z'} \left(1 - \frac{m_t^2}{M_{Z'}^2}\right) \left(1 - \frac{4m_t^2}{M_{Z'}^2}\right)^{1/2} \\ &\quad \times \left[1 + \frac{\alpha_s}{\pi} + O(\alpha_s m_t^2/M_{Z'}^2)\right] \theta(M_{Z'} - 2m_t),\end{aligned}\quad (2.13)$$

where ‘‘jets’’ refers to hadrons not containing bottom or top quarks and we have included the leading QCD corrections, but we have ignored electroweak corrections and all fermion masses with the exception of the top-quark mass,  $m_t$ . Additional decay modes, into pairs of Higgs bosons (if  $z_{H_1} \neq 0$  or  $z_{H_2} \neq 0$ ),  $CP$ -even components of the  $\phi$  scalar, right-handed neutrinos, or other new particles might be kinematically accessible and large. Therefore, the total decay width,  $\Gamma_{Z'}$ , is larger than or equal to the sum of the seven decay widths shown in Eqs. (2.12) and (2.13).

Assuming that the decays into particles other than the SM fermions are either invisible or have negligible branching ratios, the  $Z'$  properties depend primarily on 11 parameters: mass ( $M_{Z'}$ ), total width ( $\Gamma_{Z'}$ ), and nine fermion couplings  $(z_{e_j}, z_{l_j}, z_q, z_u, z_d) \times g_z$ .

### C. Realistic models

So far we have imposed  $SU(3)_C \times SU(2)_W \times U(1)_Y \times U(1)_z$  gauge invariance on the Lagrangian. Additional restrictions need to be imposed in order to preserve gauge invariance in the full quantum field theory: the fermion content of the theory has to be such that all gauge anomalies cancel. In our case, we need to make sure that there are no gauge anomalies due to triangle diagrams with gauge bosons as external lines.

Triangle diagrams involving two gluons or two  $SU(2)_W$  gauge bosons, and one  $U(1)_z$  gauge bosons give rise to the  $[SU(3)_C]^2 U(1)_z$  and  $[SU(2)_W]^2 U(1)_z$  anomalies:

$$A_{33z} = 3(2z_q - z_u - z_d), \quad A_{22z} = 9z_q + \sum_{j=1}^3 z_{l_j}.\quad (2.14)$$

Triangle diagrams involving  $U(1)_Y \times U(1)_z$  gauge bosons give rise to the  $[U(1)_Y]^2 U(1)_z$ ,  $U(1)_Y [U(1)_z]^2$  and  $[U(1)_z]^3$  anomalies:

$$\begin{aligned}A_{11z} &= 2z_q - 16z_u - 4z_d + 2 \sum_{j=1}^3 (z_{l_j} - 2z_{e_j}), \\ A_{1zz} &= 6(z_q^2 - 2z_u^2 + z_d^2) - 2 \sum_{j=1}^3 (z_{l_j}^2 - z_{e_j}^2), \\ A_{zzz} &= 9(2z_q^3 - z_u^3 - z_d^3) + \sum_{j=1}^3 (2z_{l_j}^3 - z_{e_j}^3) - \sum_{i=1}^n z_{\nu_i}^3,\end{aligned}\quad (2.15)$$

where we have included  $n$  right-handed neutrinos of charges  $z_{\nu_i}$  under  $U(1)_z$ . Finally, triangle diagrams involving two gravitons and one  $U(1)_z$  gauge boson contribute to the mixed gravitational- $U(1)_z$  anomaly, which makes general coordinate invariance incompatible with  $U(1)_z$  gauge invariance:

$$A_{GGz} = 9(2z_q - z_u - z_d) + \sum_{j=1}^3 (2z_{l_j} - z_{e_j}) - \sum_{i=1}^n z_{\nu_i}\quad (2.16)$$

Gauge invariance at quantum level requires that all the anomalies listed in Eqs. (2.14), (2.15), and (2.16) vanish, or are exactly canceled by anomalies associated with some new fermions charged under both the SM gauge group and  $U(1)_z$ . The impact of the new fermions on the  $Z'$  properties described here can be ignored if they are heavier than the  $Z'$ . Altogether, there are six equations that restrict the nine  $z$ -charges of the SM fermions. Finding solutions to this set of equations is a nontrivial task, especially if one imposes that the charges are rational numbers, as suggested by grand unified theories.

The case where the top-quark mass is generated by a Yukawa coupling to a Higgs-doublet, as in the SM or the

Minimal Supersymmetric Standard Model (MSSM), leads to Eq. (2.10), in which case the  $A_{33z}$ ,  $A_{22z}$  and  $A_{11z}$  anomalies vanish only if

$$z_q = z_u = z_d = -\frac{1}{9} \sum_{j=1}^3 z_{l_j}, \quad (2.17)$$

$$\sum_{j=1}^3 (z_{l_j} - z_{e_j}) = 0. \quad (2.18)$$

The remaining anomaly cancellation conditions, in the absence of exotic fermions, take the following form:

$$\begin{aligned} \sum_{j=1}^3 (z_{l_j}^2 - z_{e_j}^2) &= 0, \\ \sum_{j=1}^3 (2z_{l_j}^3 - z_{e_j}^3) &= \sum_{i=1}^n z_{\nu_i}^3, \quad \sum_{i=1}^n z_{\nu_i} = -9z_q \end{aligned} \quad (2.19)$$

It is hard to find general solutions to this set of equations. A well-known nontrivial solution is  $n = 3$  and  $z_{l_j} = z_{e_j} = z_{\nu_j} = z_l$ ,  $j = 1, 2, 3$ , which corresponds to the  $U(1)_{B-L}$  gauge group. The associated gauge boson,  $Z_{B-L}$ , is an interesting case of a ‘‘nonexotic’’  $Z'$  [5] relevant for Tevatron searches. We have found a generalization of this solution which preserves the  $z_{l_j} = z_{e_j} = z_{\nu_j}$  equalities within each generation, but have different lepton charges for different generations. In particular, the case of  $z_{l_1} = 0$  is worth special attention because the  $Z'$  does not couple to electrons, so there are no tight limits from LEP. In this case there are only two independent charges:  $z_q$  which sets all quark charges, and  $z_{l_2}$  which sets the charges of the muon and second-generation neutrinos. Normalizing the gauge coupling such that  $z_q = 1/3$ , the  $\tau$  and third-generation neutrinos have charge

$$z_{l_3} = -3 - z_{l_2}. \quad (2.20)$$

If new fermions are included, the anomaly cancellation conditions have more solutions. We have found that including within each generation two fermions,  $\psi^l$  and  $\psi^e$ , which under the SM gauge group are vectorlike and have the same charges as  $l_L$  and  $e_R$ , respectively, allows  $z$  charges proportional to  $B - xL$  with  $x$  arbitrary. The  $U(1)_{B-xL}$  charges are shown in Table I. This is the most general generation-independent charge assignment for the SM fermions that allows quark and lepton masses from Yukawa couplings, and is relevant for  $Z'$  searches at the Tevatron.

All other generation-independent  $U(1)_z$  charge assignments require the restrictions on fermion charges from fermion mass generation to be lifted, for example, by replacing the Yukawa couplings with higher-dimensional

operators. The six anomalies given in Eqs. (2.14), (2.15), and (2.16) vanish only for the nonexotic family of  $U(1)_z$  charges that depends on two parameters [5]. Assuming that  $z_q \neq 0$ , and normalizing the  $g_z$  gauge coupling such that  $z_q = 1/3$ , determines all other charges as a linear function of a single free parameter,  $x$ , as shown in Table I. We label this charge assignment by  $U(1)_{q+xu}$ . Particular cases of  $Z'$  ‘‘models’’ include  $U(1)_{B-L}$  for  $x = 1$ , the  $U(1)_\chi$  from  $SO(10)$  grand unification for  $x = -1$ , and the  $[U(1)_R \times U(1)_{B-L}]/U(1)_Y$  group from left-right symmetric models for  $x = 4 - 3g_R^2/g_Y^2$  where  $g_R$  is the  $U(1)_R$  gauge coupling.

Many popular  $Z'$  models are accessible at the Tevatron provided both the restrictions from fermion mass generation are lifted and new fermions charged under the SM gauge group are present. We have found a couple of generation-independent charge assignments that depend on a free parameter  $x$ , which include the  $E_6$ -inspired  $Z'$  models that have been frequently analyzed by experimental collaborations. Both require within each generation two fermions,  $\psi^l$  and  $\psi^d$ , which under the SM gauge group are vectorlike and have the same charges as  $l_L$  and  $d_R$ , respectively. One assignment, labeled by  $U(1)_{d-xu}$ , has  $z_q = 0$ ,  $z_d = 1/3$  and  $z_u = -x/3$ . For  $x = 0$  the  $E_6$ -inspired  $U(1)_I$  is recovered, while  $x = 1$  gives the ‘‘right-handed’’  $U(1)_R$  group. The other assignment is such that all fermions belonging to the 10 representation of the  $SU(5)$  grand unified group have the same  $U(1)_z$  charge, assumed to be nonzero and normalized to  $1/3$ , while the fermions belonging to the  $\bar{5}$  representation have charge  $x/3$ . We label this assignment by  $U(1)_{10+x\bar{5}}$ . Anomaly cancellation requires two right-handed neutrinos per generation. Particular  $E_6$ -inspired cases include  $U(1)_\psi$  for  $x = 1$ ,  $U(1)_\chi$  for  $x = -3$ , and  $U(1)_\eta$  for  $x = -1/2$ . Note that when the LEP and Tevatron experimental collaborations refer to these particular models, the gauge coupling is usually assumed to be determined by a unification relation:  $g_z^2 = g_Y^2 \xi$ , with  $\xi = 5/8$  for  $U(1)_\psi$ ,  $\xi = 3/8$  for  $U(1)_\chi$ ,  $\xi = 1$  for  $U(1)_\eta$ ,  $\xi = 5/3$  for  $U(1)_I$ . Thus, our families of models completely describe the physics of the grand unified theory (GUT)-inspired  $U(1)$ 's, but also allow one to relax their assumptions and explore more general  $Z'$  physics.

There is an interesting class of  $Z'$  models in which the Higgs is a pseudo-Goldstone boson of a spontaneously broken global symmetry. These ‘‘Little Higgs’’ models always include at least one  $Z'$  to cancel the leading quadratic divergence in the Higgs mass from loops of the ordinary  $W$  and  $Z$ . A prototypical model of this type is the ‘‘Littlest Higgs’’ [12]. This already reveals a key feature of the little Higgs  $Z'$ : it always couples to the Higgs, and thus generically has strong constraints from  $Z$ - $Z'$  mixing, requiring the  $Z'$  mass to be larger than several hundred GeV [13]. Thus, it is usually not very interesting for Tevatron searches.

TABLE I. Fermion gauge charges.

	SU(3) <sub>C</sub>	SU(2) <sub>W</sub>	U(1) <sub>Y</sub>	U(1) <sub>B-xL</sub>	U(1) <sub>q+xu</sub>	U(1) <sub>10+x<math>\bar{5}</math></sub>	U(1) <sub>d-xu</sub>
$q_L$	3	2	1/3	1/3	1/3	1/3	0
$u_R$	3	1	4/3	1/3	$x/3$	-1/3	$-x/3$
$d_R$	3	1	-2/3	1/3	$(2-x)/3$	$-x/3$	1/3
$l_L$	1	2	-1	$-x$	-1	$x/3$	$(-1+x)/3$
$e_R$	1	1	-2	$-x$	$-(2+x)/3$	-1/3	$x/3$
$\nu_R$	1	1	0	-1	$(-4+x)/3$	$(-2+x)/3$	$-x/3$
$\nu'_R$				...	...	$-1-x/3$	...
$\psi_L^j$	1	2	-1	-1	...	$-(1+x)/3$	$-2x/5$
$\psi_R^j$				$-x$	...	2/3	$(-1+x/5)/3$
$\psi_L^e$	1	1	-2	-1	...	...	...
$\psi_R^e$				$-x$	...	...	...
$\psi_L^d$	3	1	-2/3	...	...	-2/3	$(1-4x/5)/3$
$\psi_R^d$				...	...	$(1+x)/3$	$x/15$

#### D. LEP-II limits on $Z'$ models

The constraints from  $e^+e^-$  colliders on the  $Z'$  properties fall into two categories: precision measurements at the  $Z$  pole, through the  $Z$ - $Z'$  mixing discussed previously, and measurements of  $e^+e^- \rightarrow f\bar{f}$  above the  $Z$ -pole at LEP-II, where  $f$  are various SM fermions. In practice, the agreement with the SM requires that either the  $Z'$  gauge coupling is smaller than or of order  $10^{-2}$  [5], or else  $M_{Z'}$  is larger than the largest collider energy of LEP-II, of about 209 GeV. In the latter case, of interest at the Tevatron, one can perform an expansion in  $s/M_{Z'}^2$ , where  $s$  is the square of the center-of-mass energy. This leads to effective contact interactions which have been bounded by LEP-II for all possible chiral structures and for various combinations of fermions. These interactions are parameterized by the LEP electroweak working group [14] as,

$$\frac{\pm 4\pi}{(1 + \delta_{ef})(\Lambda_{AB}^{f\pm})^2} (\bar{e}\gamma_\mu P_A e)(\bar{f}\gamma^\mu P_B f) \quad (2.21)$$

where  $P_A$  is a projector for right- ( $A = R$ ) or left-handed ( $A = L$ ) chiral fields, and  $\delta_{ef} = 1, 0$  for  $f = e, f \neq e$ , respectively. These contact interactions provide a model-independent framework in which LEP-II data can confront high mass effects beyond the SM, up to corrections of order  $s/M_{Z'}^2$ .

In the absence of flavor violation in the  $Z'$  couplings, the  $Z'$  contributions to  $e^+e^- \rightarrow f\bar{f}$  for  $f \neq e$  proceed through an  $s$ -channel  $Z'$  exchange, with tree level matrix element,

$$\frac{g_z^2}{M_{Z'}^2 - s} [\bar{e}\gamma_\mu (z_L P_L + z_R P_R) e][\bar{f}\gamma^\mu (z_{fL} P_L + z_{fR} P_R) f] \quad (2.22)$$

where tiny terms of order  $m_f m_e / M_{Z'}^2$  have been dropped. In the case of  $f = e$ , there is also a  $t$ -channel exchange, which in fact motivates the factor of  $(1 + \delta_{ef})$  in Eq. (2.21), which allows one to treat all  $f$  equivalently at the level of matrix elements.

One should compare the LEP  $\Lambda_{LL}, \Lambda_{RR}, \Lambda_{LR},$  and  $\Lambda_{RL}$  limits to the operators of each structure in the  $Z'$  theory in order to find a limit on a given  $Z'$  model. This procedure finds the best *single* bound from each operator on a given  $Z'$  model, but it ignores the potentially stronger bound that comes from the combined effect of more than one operator. In the absence of a dedicated reanalysis of the data, this is the best one may do. However, we reiterate that it does not always represent the best potential bound from the data, due to correlated effects on observables which cannot be taken into account correctly in this way. Typically the strongest bound comes from a single choice of chiral interaction combination and  $f$ .

Matching the  $Z'$  matrix elements, Eq. (2.22), to the LEP-II formalism, Eq. (2.21), one derives bounds such as,

$$M_{Z'}^2 - s \geq \frac{g_z^2}{4\pi} |z_{e_A} z_{f_B}| (\Lambda_{AB}^{f\pm})^2, \quad (2.23)$$

and one must choose  $\Lambda^+$  for  $z_{e_A} z_{f_B} > 0$  or  $\Lambda^-$  for  $z_{e_A} z_{f_B} < 0$ . Typically, the LEP-II bounds on the  $\Lambda$ 's are on the order of 10 TeV, schematically translating into bounds on the  $Z'$

mass on the order of  $M_{Z'} \gtrsim |z| g_z \times (\text{a few TeV})$ . More precise bounds in the case of certain models are discussed below. The Tevatron can effectively improve our knowledge of  $Z'$  models only when the couplings  $z g_z$  are appropriately small such that the LEP-II limits are evaded for  $Z'$  masses in the several hundred GeV range, but large enough that the  $Z'$  rate is observable compared to backgrounds.

For example,  $U(1)_{B-xL}$  has vectorlike interactions with quarks and leptons, and thus it is better to compare LEP limits for vectorlike interactions ( $\Lambda_{VV}$ ) than for the individual chiral set of  $\Lambda_{LL}$ ,  $\Lambda_{RR}$ ,  $\Lambda_{LR}$ , and  $\Lambda_{RL}$ . From Ref. [14], we see that the strongest of the  $\Lambda_{VV}^+$  bounds is from the process  $e^+e^- \rightarrow \ell^+\ell^-$ :  $\Lambda^+ > 21.7$  TeV. This is in fact one of the most stringent bounds to be found from LEP-II. Translating this bound in the specific couplings of  $U(1)_{B-xL}$  results in the limit  $M_{Z'} \geq |x|g_z \times (6 \text{ TeV})$ . For the remaining models of Table I, the analysis is more complicated, because the best bounded channel typically depends on the value of  $x$ . Thus, for these models, we have scanned (for fixed  $-10 \leq x \leq 10$ ) through all channels of  $\Lambda_{LL}$ ,  $\Lambda_{RR}$ ,  $\Lambda_{LR}$ ,  $\Lambda_{RL}$  and chosen the best bound. The results are shown in Fig. 1. It is interesting to note that for  $|x| \gtrsim 1$ ,  $U(1)_{B-xL}$  is very strongly constrained by LEP-II data, whereas for  $x \rightarrow 0$  the coupling to electrons becomes small and the bounds disappear.

We have compared our results for general  $x$  with the  $E_6$ -inspired models studied in detail at LEP-II [14]. As explained above, these correspond to specific points in  $x$  for a given model family. We find that our results agree with the LEP bounds for the dedicated analysis at or better than the 25% level (depending on the model), thus indicating that our procedure does a good job in comparison with the dedicated analysis for the points in which the two may be compared. For most of the parameter space there is no dedicated LEP analysis, and we

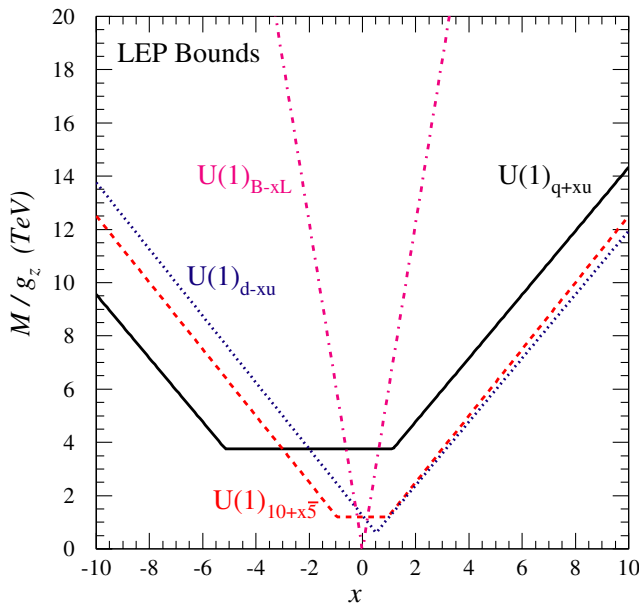


FIG. 1 (color online). Lower bounds on  $M_{Z'}/g_z$  from the LEP-II search for  $LL$ ,  $RR$ ,  $LR$  and  $RL$  contact interactions, applied to the models of Table I as a function of the continuous parameter  $x$ . For  $U(1)_{B-xL}$ , we have included the bound on vectorlike  $e^+e^- \rightarrow \ell^+\ell^-$ , as is appropriate for that model.

present for the first time the LEP bounds on the general class of  $Z'$  models.

Generically, the fact that LEP-II was an  $e^+e^-$  collider implies that these strong bounds can be evaded by a  $Z'$  which couples only very weakly to electrons.<sup>2</sup> Also, different chiral structures than the vectorlike interactions of  $U(1)_{B-xL}$  can have weaker bounds. From Ref. [14] one observes that a  $Z'$  which couples only to left-handed or right-handed electrons is bounded only by  $\Lambda^+ \geq 7.1, 7.0$  TeV (for  $\Lambda_{LL}$  and  $\Lambda_{RR}$ , respectively). This implies a bound of  $M_{Z'} \geq g_{z\bar{z}} \times (1.9 \text{ TeV})$ , approximately 3 times weaker than the bound on  $U(1)_{B-xL}$ .

### III. Z' SEARCHES AT THE TEVATRON

At the Tevatron, searches for additional neutral gauge bosons can be performed in a variety of processes. If such bosons couple to the SM quarks, they may be directly observed through their production and subsequent decay into high energy lepton pairs or jets. The case of the decay into leptons is particularly attractive due to low backgrounds and good momentum resolution. Bounds on several models containing extra neutral gauge bosons, have been set by both the CDF collaboration[18–20] and D0 [21–23] experiments by measuring high energy lepton pair production cross sections. Searches have been made in the  $e^+e^-$  channel, which has the best acceptance, and thus best systematics, as well as in the  $\mu^+\mu^-$  channel. More recently, the challenging  $\tau^+\tau^-$  channel has also been analyzed [24]. The  $\mu^+\mu^-$  and  $\tau^+\tau^-$  final states, along with the  $Z'$  decay into jets which suffers from huge QCD backgrounds, can probe  $Z'$  bosons with suppressed couplings to the electrons, which are not constrained by the LEP searches.

In what follows, we will restrict ourselves to the study of the leptonic decay modes, proposing a simple, model-independent, parametrization for the  $Z'$  production cross section and analyzing its theoretical and experimental feasibilities and limitations.

#### A. Z' Hadro-production

The additional terms, beyond those coming from SM particles, in the differential cross section for production of a pair of charged leptons due to the presence of an extra neutral gauge boson can be written as [25]

$$\frac{d}{dQ^2} \sigma(p\bar{p} \rightarrow Z'X \rightarrow l^+l^-X) = \frac{1}{s} \sigma(Z' \rightarrow l^+l^-) W_{Z'}(s, Q^2) + \frac{d\sigma_{\text{int}}}{dQ^2}, \quad (3.1)$$

where  $Q$  is the invariant mass of the lepton pair, and  $\sqrt{s}$  is

<sup>2</sup>For example, theories such as Top-color assisted Technicolor [15], Top-flavor [16], or Supersymmetric Top-flavor [17], have small couplings to the first generation.

the energy of the  $p\bar{p}$  collision in the center-of-momentum frame. The first term accounts for the contributions from the  $Z'$  itself and has been explicitly factorized into a hadronic structure function,  $W_{Z'}$ , containing all the QCD dependence and the couplings of quarks to the  $Z'$ , and

$$\sigma(Z' \rightarrow l^+l^-) = \frac{g_z^2}{4\pi} \left( \frac{z_{l_j}^2 + z_{e_j}^2}{288} \right) \frac{Q^2}{(Q^2 - M_{Z'}^2)^2 + M_{Z'}^2 \Gamma_{Z'}^2}. \quad (3.2)$$

Up to next-to-leading order (NLO) in QCD, only the partonic processes  $\bar{q}q \rightarrow Z'X$  (nonsinglet) and  $qg \rightarrow Z'X$  contribute to the hadronic structure function. If the  $Z'$  couplings to quarks are generation independent, both processes give contributions which are proportional to  $(z_q^2 + z_u^2)$  or  $(z_q^2 + z_d^2)$  for up and down-type quarks, respectively. Therefore, the hadronic structure function can be written as

$$W_{Z'}(s, M_{Z'}^2) = g_z^2 [(z_q^2 + z_u^2)w_u(s, M_{Z'}^2) + (z_q^2 + z_d^2)w_d(s, M_{Z'}^2)]. \quad (3.3)$$

The functions  $w_u$  and  $w_d$  do not depend on any coupling and are exactly the same for any model containing neutral gauge bosons coupled in a generation independent way to quarks. In the  $\overline{\text{MS}}$  scheme, they are given by

$$w_{u(d)} = \sum_{q=u,c(d,s,b)} \int_0^1 dx_1 \int_0^1 dx_2 \int_0^1 dz \{ f_{q/P}(x_1, M_{Z'}^2) f_{\bar{q}/\bar{P}} \times (x_2, M_{Z'}^2) \Delta_{qq}(z, M_{Z'}^2) + f_{g/P}(x_1, M_{Z'}^2) \times [f_{q/\bar{P}}(x_2, M_{Z'}^2) + f_{\bar{q}/P}(x_2, M_{Z'}^2)] \Delta_{gq}(z, M_{Z'}^2) + (x_1 \leftrightarrow x_2, P \leftrightarrow \bar{P}) \} \delta\left(\frac{M_{Z'}^2}{s} - zx_1x_2\right), \quad (3.4)$$

where  $f_{i/P}(x, M^2)$  and  $f_{i/\bar{P}}(x, M^2)$  are the PDFs for the proton and antiproton, respectively, and

$$\Delta_{qq}(z, M_{Z'}^2) = \delta(1-z) + \frac{\alpha_s(M_{Z'}^2)}{\pi} C_F \left[ \delta(1-z) \left( \frac{\pi^2}{3} - 4 \right) + 4 \left( \frac{\ln(1-z)}{1-z} \right)_{+z[0,1]} - 2(1+z) \ln(1-z) - \frac{1+z^2}{1-z} \ln z \right], \quad (3.5)$$

$$\Delta_{gq}(z, M_{Z'}^2) = \frac{\alpha_s(M_{Z'}^2)}{2\pi} T_F \left[ (1-2z+2z^2) \ln \frac{(1-z)^2}{z} + \frac{1}{2} + 3z - \frac{7}{2}z^2 \right]. \quad (3.6)$$

The color factors are  $C_F = 4/3$  and  $T_F = 1/2$ , and we have set the renormalization and factorization scales to  $M_{Z'}$ .

The second term in Eq. (3.1),  $d\sigma_{\text{int}}/dQ^2$ , corresponds to the interference of the  $Z'$  with the  $Z$  and the photon. If the  $Z'$  resonance is narrow enough, the interference of the  $Z'$  with the  $Z$  and photons can be neglected (see the Appendix).

In the narrow width approximation, the expression for the total cross section is simply obtained from the differential cross section, explicitly

$$\sigma(p\bar{p} \rightarrow Z'X \rightarrow l^+l^-X) = \frac{\pi}{48s} W_{Z'}(s, M_{Z'}^2) \text{Br}(Z' \rightarrow l^+l^-), \quad (3.7)$$

where  $\text{Br}(Z' \rightarrow l^+l^-)$  is the branching ratio for the decay of  $Z'$  into the corresponding pair of leptons. Using the expression of the hadronic structure function, Eq. (3.3), one obtains

$$\sigma(p\bar{p} \rightarrow Z'X \rightarrow l^+l^-X) = \frac{\pi}{48s} [c_u w_u(s, M_{Z'}^2) + c_d w_d(s, M_{Z'}^2)]. \quad (3.8)$$

The coefficients  $c_u$  and  $c_d$ , given by

$$c_{u,d} = g_z^2 (z_q^2 + z_{u,d}^2) \text{Br}(Z' \rightarrow l^+l^-), \quad (3.9)$$

contain all the dependence on the couplings of quarks and leptons to the  $Z'$ , while  $w_u$  and  $w_d$  only depend on the mass of the gauge boson and can be calculated in a completely model-independent way.

The parametrization given in Eq. (3.8) permits a direct extraction of a bound in the  $c_u - c_d$  plane from the experimental limit for the cross section, which can be later compared to the predictions of particular models. This fact is particularly useful for models admitting free parameters like the ones discussed in the preceding sections. In particular, these quantities are simply computed for a given  $Z'$  model, without need to compute the hadro-production cross section, and thus are a common ground between theory and experiment.

The D0 and CDF Collaborations have set preliminary 95% C.L. limits for  $\sigma \cdot \text{Br}(Z' \rightarrow l^+l^-)$  in Run II with 200 fb<sup>-1</sup> [26,27]. In Fig. 2 we show the excluded regions in the  $c_d - c_u$  plane for different values of the mass of the  $Z'$  boson as obtained from the limit on  $\sigma \cdot \text{Br}(Z' \rightarrow l^+l^-)$  given by the CDF Collaboration [27] in Run II with 200 fb<sup>-1</sup>. Very similar results are obtained using the results by the D0 Collaboration [26]. The  $w_u$  and  $w_d$  coefficients in Eq. (3.8) for this plot were calculated at NLO with MRST02 PDFs [28]. From the current generation of CTEQ [29] parton distribution functions (PDF), one obtains very similar results.

It is instructive to compare these limits with the predictions of the four families of models presented in Sec. II. The values of  $c_u$  and  $c_d$  as functions of the gauge coupling  $g_z$  and the  $x$  parameter are given in Table II. Figure 2 displays the values of  $(c_d, c_u)$  corresponding to the  $B - xL$  and  $q + xu$  models. In the  $B - xL$  case, these

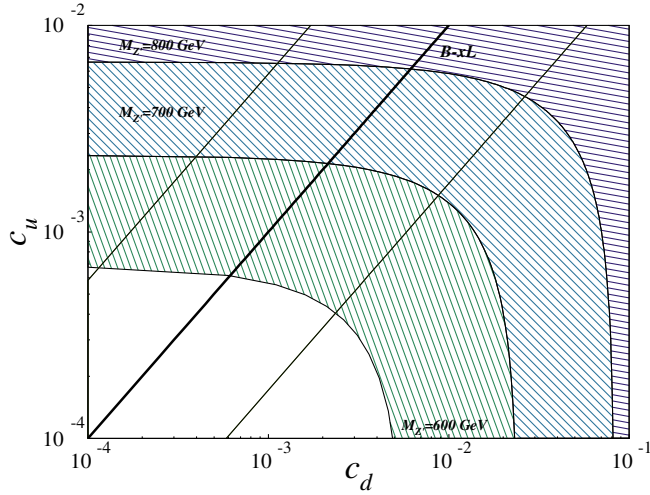


FIG. 2 (color online). Excluded regions in the  $c_d - c_u$  plane from the current 95% C.L. limit for  $\sigma \cdot \text{Br}(Z' \rightarrow l^+ l^-)$  given in [27], for different values of the  $Z'$  mass. The thick straight line corresponds to values of  $c_u$  and  $c_d$  in the  $B - xL$  model, in which  $c_u = c_d$ . The area between the two thin straight lines is the region where the  $q + xu$  model lies.

points are constrained to satisfy  $c_u = c_d$ , corresponding to the thick straight line. For the  $q + xu$  model, the allowed region is

$$(3 - 2\sqrt{2})c_d \leq c_u \leq (3 + 2\sqrt{2})c_d, \quad (3.10)$$

which corresponds to the area between the two thin straight lines in Fig. 2. The  $10 + x\bar{5}$  model, in turn, is constrained to the region  $c_u \leq 2c_d$ , whereas there are no constraints for the possible values of  $c_d$  and  $c_u$  in the  $d - xu$  model.

### B. Higher-order corrections

At next-to-next-to-leading order (NNLO) in QCD, the general expression in Eq. (3.3) is no longer valid. This is due to the contributions from the partonic processes  $\bar{q}q \rightarrow Z'X$  (singlet) and  $qq \rightarrow Z'X$ , which depend upon a variety of coupling combinations in addition to  $(z_q^2 + z_u^2)$  and  $(z_q^2 + z_d^2)$ . Thus, one should worry whether  $c_u$  and  $c_d$  are a sufficient description of the model. The actual size of these corrections can be estimated by looking at a particular model. In Fig. 3 we plot the sizes of the  $\mathcal{O}(\alpha_s)$  and  $\mathcal{O}(\alpha_s^2)$  terms to the structure function at NNLO relative to

TABLE II. Predictions for  $c_d$  and  $c_u$  in four families of models defined in Table I. The branching fractions are computed at tree level for  $M_{Z'} > 2m_l$ , and assuming decays only into SM particles.

	$U(1)_{B-xL}$	$U(1)_{q+xu}$	$U(1)_{10+x\bar{5}}$	$U(1)_{d-xu}$
$c_u/g_z^2$	$\frac{4x^2}{9(4+9x^2)}$	$\frac{(1+x^2)(13+4x+x^2)}{27(40-8x+7x^2)}$	$\frac{2(1+x^2)}{135(2+x^2)}$	$\frac{x^2(1-2x+2x^2)}{27(5-4x+6x^2)}$
$c_d/c_u$	1	$1 + 4\frac{1-x}{1+x^2}$	$\frac{1+x^2}{2}$	$\frac{1}{x^2}$

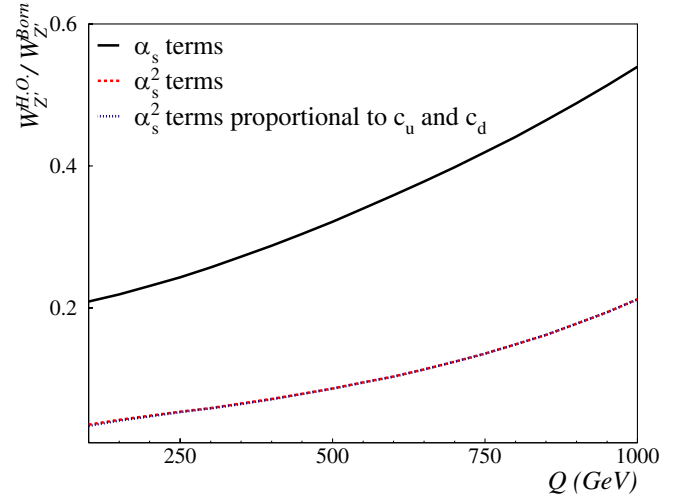


FIG. 3 (color online). The ratio of the  $\mathcal{O}(\alpha_s)$  and  $\mathcal{O}(\alpha_s^2)$  corrections to the hadronic structure function over the Born contribution, assuming SM couplings for the  $Z'$ . The full line corresponds to the  $\mathcal{O}(\alpha_s)$  corrections. The dashed and dotted lines, which, within the resolution of the figure, appear as a single line, correspond to the total  $\mathcal{O}(\alpha_s^2)$  contributions and to the  $\mathcal{O}(\alpha_s^2)$  corrections retaining only those terms that give contributions proportional to  $c_u$  and  $c_d$  to the cross section, respectively.

the Born contribution for the case of SM-like couplings of the  $Z'$  boson. The NNLO corrections were calculated with the program ZPROD [25,30,31] and the MRST02 NNLO set of PDFs [28]. We have split the  $\mathcal{O}(\alpha_s^2)$  corrections in two parts, one proportional to  $c_d$  and  $c_u$ , and the other depending upon other combinations of the couplings. Contributions proportional to  $c_d$  and  $c_u$ , coming from  $\mathcal{O}(\alpha_s^2)$  corrections to processes already present at lower orders, are clearly the dominant ones, overcoming the remaining pieces by more than an order of magnitude in the whole  $Q$  range. Typically the terms with mixed couplings contribute less than one per mil to the structure function, while the total  $\mathcal{O}(\alpha_s^2)$  corrections amount between 2% and 20% [for comparison, the  $\mathcal{O}(\alpha_s)$  terms contribute between 20% and 50% of the structure function].

Although the actual values of the different higher-order corrections will depend upon the model considered, it is reasonable to expect that terms not contributing to the  $c_d$ - $c_u$  piece of the cross section will be negligible at NNLO. In that case, the parametrization in Eq. (3.3) holds as a very good approximation, and experimental bounds can be set in a model-independent way, taking  $c_d$ ,  $c_u$  and  $M_{Z'}$  as the only relevant parameters at NNLO accuracy.

It is customary to take into account higher-order corrections to the structure function by means of a  $k$ -factor, allowing the use of LO Montecarlo simulations, corrected afterwards by the mentioned factors. As the struc-

ture function at LO has a different dependence upon  $Q$  than at NLO or NNLO, the corresponding  $k$ -factors, defined as the ratio of the higher-order results over the LO one,  $k_{N^i\text{LO}} = W_{Z'}^{N^i\text{LO}}/W_{Z'}^{\text{LO}}$ , vary noticeably with the invariant mass of the lepton pair. This variation has to be properly taken into account when correcting LO Montecarlo results.

In Fig. 4 we plot the NLO and NNLO  $k$ -factors obtained again with the program ZPROD, for SM-like couplings. There, we also show a usual approximation for the NLO  $k$ -factor (used, for instance, in Ref. [20]), which takes into account only the soft pieces of the NLO structure function in the deeply inelastic scattering scheme, namely

$$k_{\text{soft}} = 1 + \frac{4}{3} \frac{\alpha_s(Q^2)}{2\pi} \left(1 + \frac{4}{3} \pi^2\right). \quad (3.11)$$

The variation of the  $k$ -factor, in the plotted range of  $Q$ , for the NLO case amounts to more than 10%, the genuinely NNLO corrections are also sizable whereas the soft approximation does not provide a good description of the higher-order effects. The difference between the soft approximation and the full  $k$ -factors, yields a discrepancy of about 5% to 10% for the cross section in the high mass region, which is particularly relevant in the search of extra gauge bosons. Similar results are obtained using a flat  $k$ -factor with  $k = 1.3$ , as in Ref. [27], instead of the soft approximation.

So far we only discussed QCD corrections to the  $Z'$  cross section, which are of the order of 30% as can be seen from the  $k$ -factors in Fig. 4. There are also corrections from the electroweak sector, which we will address briefly. The complete  $\mathcal{O}(\alpha)$  corrections to the SM contri-

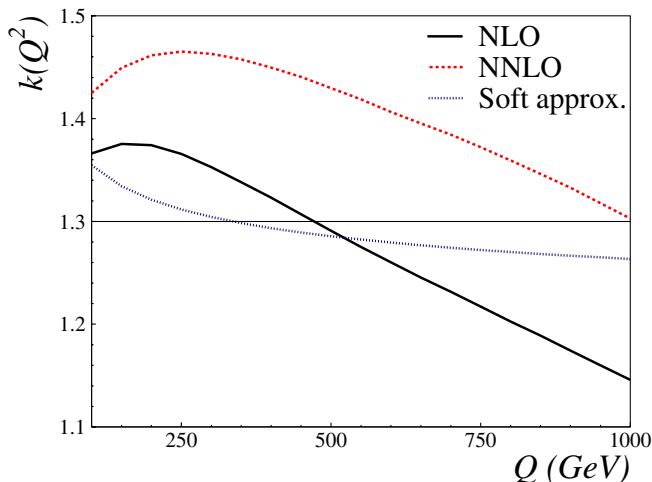


FIG. 4 (color online). NLO and NNLO  $k$ -factors for SM-like couplings as a function of the invariant mass of the lepton pair. Also shown is an approximation, Eq. (3.11), for the NLO  $k$ -factor which only takes into account the soft corrections to the structure function in the deeply inelastic scattering scheme.

butions to neutral current Drell-Yan process were calculated in [32]. There, it was found that these corrections are large, particularly in the high invariant mass region, being of the order of 12% at Tevatron energies for  $m_{ll} \simeq 700$  GeV in the electron channel. Besides affecting the background for the search of additional neutral gauge bosons, electroweak radiative corrections also modify the signal cross section. However, as we will see, these effects are substantially smaller for the  $Z'$  terms.

As shown in [32], the main contributions to the electroweak corrections come from the box diagrams and cannot be factorized into effective couplings and masses. In particular, box diagrams with two charged bosons give rise to large double logarithms which are the origin of the large corrections in the high mass region. On the other hand, box diagrams that include neutral bosons ( $\gamma$ ,  $Z^0$  and  $Z'$ ) always appear in combination with their crossed versions and that leads to a cancellation of the double logs [33]. Then, the nonfactorizable contributions that affect exclusively the signal cross section only include subleading simple logs and thus the corrections are expected to be smaller than for the SM background.

The remaining contributions come from QED and factorizable purely weak corrections. The later can always be absorbed into effective couplings and masses, thus, they do not affect the signal cross section where these quantities are treated as free parameters. The main electromagnetic contributions come from large logarithms due to collinear photon emission in the initial and final states, and affect both the signal and background cross sections. The large contributions coming from initial state radiation can be factorized into the PDFs, modifying the Dokshitzer-Gribov-Lipatov-Altarelli-Paraisi evolution equations for the partonic densities. After factorization, the remaining terms are typically at the per mil level, reaching 1% in the high momentum fraction region [32] whereas the QED modifications to the evolution equations are small and neglected in comparison to the uncertainties in the PDFs [34]. However, collinear emission in the final state gives corrections of the order of 5% for the electron channel in the high mass region, and a careful analysis should probably take them into account.

### C. Model dependence in experimental bounds

As we have shown in the previous section, the parametrization given in Eq. (3.8) allows to extract model-independent constraints on the coefficients  $c_d$  and  $c_u$  from the experimental results for the lepton pair production cross section. A key assumption for this analysis is that the bounds for the cross section can be extracted from data in a model-independent manner. In particular, the experimental analyses involve corrections for the finite acceptance of the detectors to extract the total cross section. As the acceptance is obtained from detailed

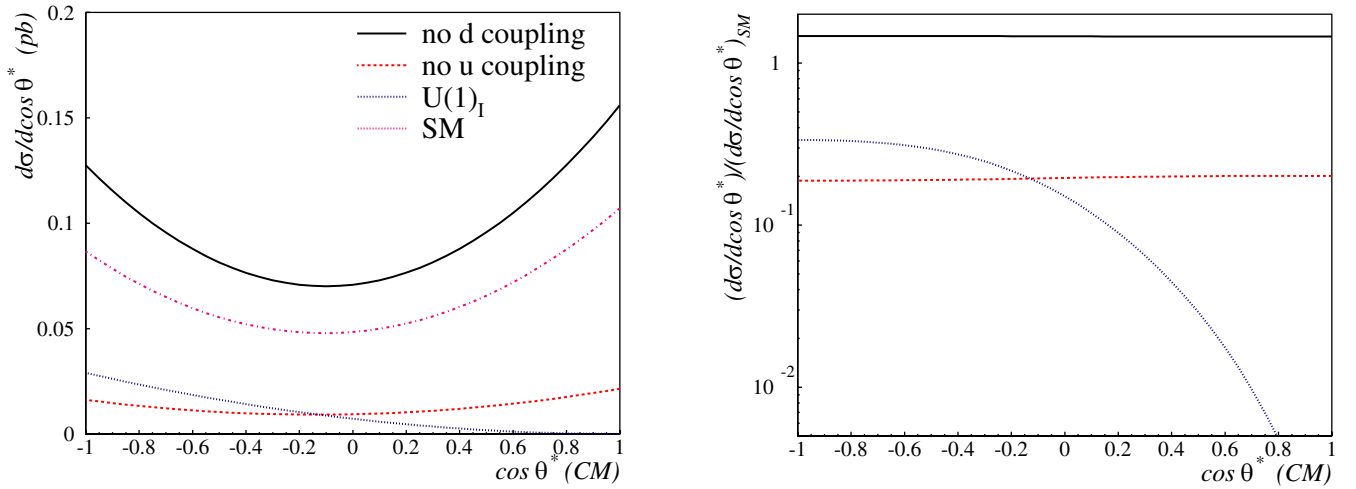


FIG. 5 (color online). (a) Angular distribution, in the CM frame of the lepton pair, at LO in QCD for different models. The lines labeled no  $u$  ( $d$ ) coupling correspond to SM charges but neglecting the coupling of up (down) type quarks to the  $Z'$ . (b) Ratio between the differential cross section (shown in panel a) in different models and the case of SM-like charges.

Monte Carlo simulations, which need to assume particular values of the couplings, it is far from trivial that this procedure does not introduce model dependence into the experimental bounds.

In Ref. [18], the changes in the acceptance with variations in the couplings of up and down quarks were studied. There, it was found that the acceptance changes very little when considering the limiting cases of either decoupling up or down quarks. However, this study was limited to SM-like couplings for electrons, a feature that, *a priori*, might be too restrictive. To study the actual model dependence of the experimental acceptance, in this section, we will consider the angular distribution of the lepton pair and apply simple cuts on this distribution. For simplicity we will restrict to the LO approximation.

In the left panel of Fig. 5 we plot the LO cross section differential with respect to the azimuthal angle, in the center of mass frame of the lepton pair, with different assumptions for the couplings, setting  $M_{Z'} = 600$  GeV. We considered SM-like couplings, SM-like couplings with up or down couplings neglected, and the  $E_6$  inspired model  $U(1)_I$  mentioned in Sec. II. The right panel shows the ratios between the cross section in the last three cases to the cross section with SM couplings. Except for the overall normalization, the cases where the  $Z'$  does not couple to either up or down-type quarks differ very little from the SM case. This feature can be traced back to the peculiar fact that, in the SM, the left and right-handed couplings of charged leptons, satisfy  $z_l^2 - z_e^2 = \sin^2\theta_W - 1/4 \approx 0.02$ . Then, the terms odd under  $\theta \rightarrow -\theta$  are suppressed relative to the even ones in the LO differential cross section, which turns out to be nearly symmetric. This characteristic feature is in sharp contrast with the behavior in the  $U(1)_I$  case, where the asymmetry is almost maximal. This is related to the vanishing of the

couplings of the right-handed electrons and left-handed down-type quarks to the  $Z'$  in this last model.

To get a handle on how the noticeable differences in the angular distribution affect the experimental acceptance, we crudely estimated it by integrating the differential cross section imposing a symmetric cut on the lepton angle, defined in the laboratory frame, and normalizing to the total cross section. In Fig. 6 we plot the results obtained for the models considered in the previous paragraph, taking the  $U(1)_I$  case as reference normalization.

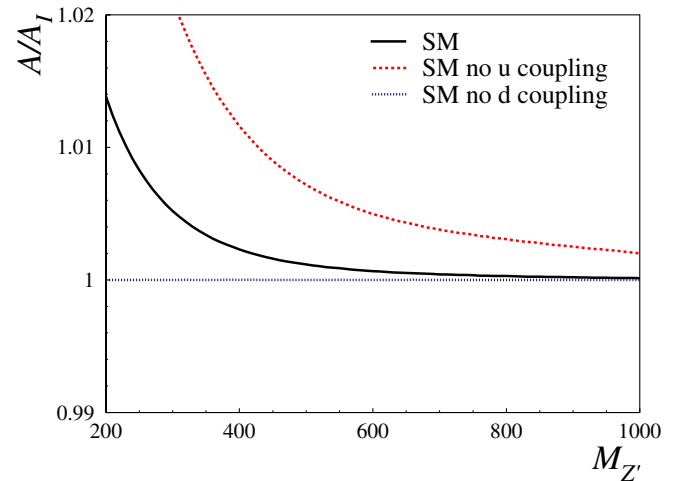


FIG. 6 (color online). The Acceptance ( $A$ ), computed from the LO cross section integrated over the azimuthal angle of the leptons in the laboratory frame in the region  $50^\circ \leq \theta_{\text{lab}} \leq 130^\circ$ . We considered the cases of SM couplings, SM couplings without  $u$ -quark couplings and without  $d$ -quark couplings, respectively. To show the variation compared to a most extreme situation, we normalize to the corresponding LO acceptance of the  $U(1)_I$  model.

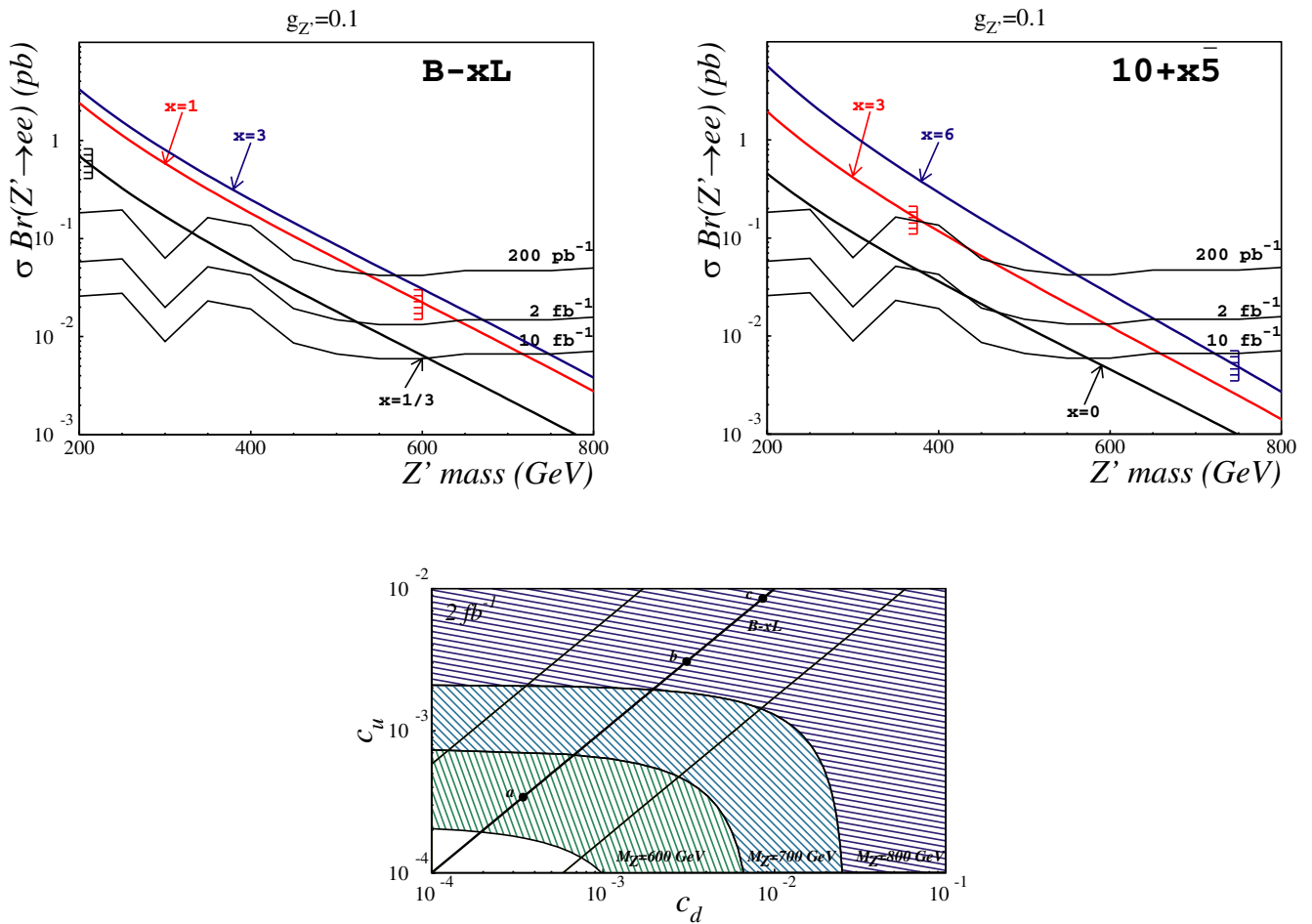


FIG. 7 (color online). Projected bounds for the  $B - xL$  (left upper panel) and  $10 + x\bar{5}$  (right upper panel) models and projected excluded regions in the  $c_d - c_u$  plane (lower panel). In the two upper panels, the vertical marks show the current LEP bounds for the  $Z'$  mass obtained as described in Sec. II C. In the  $B - xL$  case, for  $x = 3$  this last bound is  $M_{Z'} \geq 1800$  GeV; for the  $10 + x\bar{5}$ , the bound for  $x = 0$  is  $M_{Z'} \geq 119$  GeV, beyond the scope of the figure. The projected bounds at luminosities  $\mathcal{L} = 2 \text{ fb}^{-1}$ ,  $10 \text{ fb}^{-1}$  are obtained from Fig. 2 by scaling with a factor  $1/\sqrt{\mathcal{L}}$ . The lower panel also shows the regions in the  $c_d - c_u$  plane corresponding to the  $B - xL$  and  $q + xu$  models, as in Fig. 2, showing the projected increase in reach with two  $\text{fb}^{-1}$ . The dots labeled  $a$ ,  $b$  and  $c$  correspond to the  $B - L$  model with  $g_z = 0.1$ ,  $g_z = 0.3$  and  $g_z = 0.5$ , respectively.

Although the angular distribution in this model differs substantially from that in the other cases, the corresponding acceptances coincide at the few percent level. Note that the SM case without down-type quark couplings is practically indistinguishable from the  $U(1)_I$  one.

This, apparently peculiar, result for the acceptance is due to the fact that, on average, the vector boson is produced with very small longitudinal momentum, so the boost to go from the laboratory frame to the center of mass one is small. Thus, a symmetric cut in the lab frame corresponds to an almost symmetric cut in the center of mass frame, which in turn means that the ratio we are using to estimate the acceptance has only small contributions that depend on the couplings of the quarks and leptons to the  $Z'$ . In particular, models that do not couple at all to up (down) type quarks give practically identical results for the acceptance.

In conclusion, we find that, even though the angular distribution of the final state leptons is highly model dependent, the experimental acceptance, which we naively estimate through angular cuts, is only mildly affected by this dependence, in accordance with previous studies by the experimental groups. On the other hand, the model dependence of the angular distribution potentially can be a tool to discriminate between models in case of a discovery.

#### D. Probes of $Z'$ models at the Tevatron

With the forthcoming data, the Tevatron experiments will be able to explore a new region in masses and couplings for many models containing extra neutral bosons, with the chance of making a  $Z'$  discovery.

In case that no signal excess is observed, the extracted limits to the  $Z'$  cross section will set new bounds on masses and couplings, or alternatively on the  $c_u$  and  $c_d$  parameters discussed in previous sections. As an illustration, in Fig. 7, we show estimates for the experimental limits, for different values of the integrated luminosity. For these estimates, we considered the current CDF bound [27] and assumed that the limit scales as the inverse of the square root of luminosity, as will be the case provided the limit is dominated by statistics and not systematics. In the two upper panels, we plot the bounds on cross section times branching ratio, as a function of  $M_{Z'}$ , together with the predictions for different values of  $x$  in the  $B - xL$  (left) and in the  $10 + x\bar{5}$  (right) models. We also show the mass bounds, for the different cases, set by the LEP contact interaction constraints discussed before. The lower panel shows the excluded regions in the  $c_d - c_u$  plane for different values of the  $Z'$  mass, assuming an integrated luminosity of  $2 \text{ fb}^{-1}$ .

The results in Fig. 7 show that, both in the cases of the  $B - xL$  and  $10 + x\bar{5}$  models, there is a sizable unexplored region in parameter space that the Tevatron will certainly be able to probe. For the  $B - xL$  models, LEP bounds are stronger for larger values of  $|x|$ , while the Tevatron can do much better for  $|x| \lesssim 1$ . For the  $10 + x\bar{5}$  models, the LEP bounds are slightly weaker than in the previous case and the unbounded region in  $x$  space is larger.

If a signal excess is seen in the invariant mass distribution, it would also be possible to shed some light on the nature of the couplings of the new boson to the fermions by studying the angular distribution of the final state

leptons. As shown in the previous section, there are substantial differences, between models, in the predicted angular distribution.

In Fig. 8 we show the forward-backward asymmetry at the Tevatron, predicted in the  $B - xL$  and  $d - xu$  models for the case of a  $Z'$  boson with  $M_{Z'} = 700 \text{ GeV}$ . The shift from the SM prediction of the forward-backward asymmetry in these two models has opposite sign, allowing, in principle, to distinguish between them, provided enough statistics are collected in the high mass region. Observables at the Tevatron other than the forward-backward asymmetry are discussed in Ref. [35], while capabilities of the LHC and a high energy  $e^+e^-$  linear collider are addressed in Ref. [6].

#### IV. CONCLUSIONS

At the Tevatron, the hypothetical  $Z'$  bosons may be produced via their couplings to light quarks, and are more likely to be detected if they decay into charged leptons. The typical signature of a  $Z'$  boson would be a bump in the total cross section for dilepton production as a function of the dilepton invariant mass. The observability of a dilepton signal in the inclusive process  $p\bar{p} \rightarrow l^+l^-X$ , where  $l$  stands for  $e, \mu$  or  $\tau$ , is controlled primarily by two quantities: the  $Z'$  mass, and the  $Z'$  decay branching fraction into  $l^+l^-$  times the hadronic structure function  $W_{Z'}$  defined in Eq. (3.3). The exclusion limits presented by the D0 [21–23] and CDF Collaborations [18–20] are curves in the plane spanned by these two parameters. Such an exclusion plot is very useful, allowing one to derive the range of  $Z'$  parameters consistent with the experiment. However, the hadronic structure function entangles the model dependence contained in the quark- $Z'$  couplings with the information about the proton and antiproton structures contained in the PDFs. In order to simplify the derivation of the exclusion limits in the large  $Z'$  parameter space, we are advocating the presentation of the exclusion curve (see Fig. 3) in the  $c_u - c_d$  plane, where  $c_u$  and  $c_d$  are the decay branching fraction into leptons times the average square coupling to up and down quarks, respectively.

Assuming that the couplings of  $Z'$  to quarks and leptons are independent of the fermion generation, the  $Z'$  properties are described primarily by seven parameters: mass ( $M_{Z'}$ ), total width ( $\Gamma_{Z'}$ ), and five fermion couplings ( $z_e, z_l, z_q, z_u, z_d$ )  $\times g_z$ . The exclusion curve in the  $c_u - c_d$  plane sets a bound on a single combination of these seven parameters. Nevertheless, in any specific model defined by certain fermion charges it is straightforward to compute  $c_u$  and  $c_d$ , and to derive what is the limit on the gauge coupling  $g_z$  as a function of  $M_{Z'}$ .

For example, if the quark and lepton masses are generated by Yukawa couplings to one or two-Higgs doublets, as in the SM or its supersymmetric versions, the only gauge groups that may provide a  $Z'$  gauge boson acces-

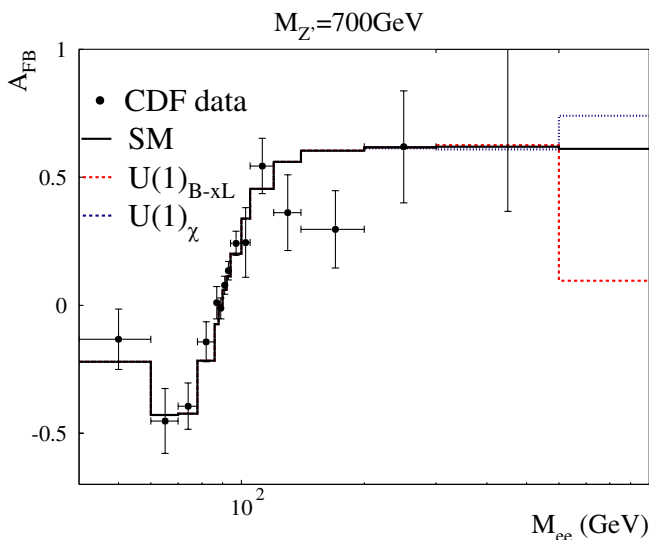


FIG. 8 (color online). The forward-backward asymmetry at LO for the  $B - L$  and  $U(1)_{d-xu}$  models with  $M_{Z'} = 700 \text{ GeV}$ . In the case of  $B - L$  we chose  $g_z = 0.1$ . For the  $U(1)_{d-xu}$  models, we fixed  $x = 1$  and  $g_z = 0.5$ . We also show the SM prediction and recent CDF data for this observable [36].

sible at the Tevatron are of the type  $U(1)_{B-xL}$ . This means that all fermion charges are determined by a single parameter,  $x$ . Within this family of gauge groups,  $c_u$  and  $c_d$  have a simple dependence on  $x$  and  $g_z$ ; for a given  $x$  and  $M_{Z'}$ , the limit on  $g_z$  can be immediately derived.

If the quark and lepton masses are generated by a more general mechanism,  $Z'$  gauge bosons associated with gauge groups other than  $U(1)_{B-xL}$  may be accessible at the Tevatron. We have presented three other examples of one-parameter families of  $U(1)$  gauge groups, chosen to include (for particular values of the parameter  $x$ ) many of the  $Z'$  models discussed in the literature. For these families of models, the Tevatron reach goes significantly beyond the LEP-II bounds for large regions of the three dimensional parameter space spanned by  $M_{Z'}$ ,  $g_z$  and  $x$ .

Relaxing the assumption that the couplings of  $Z'$  to leptons are generation-independent, for each of the  $e^+e^-$ ,  $\mu^+\mu^-$  and  $\tau^+\tau^-$  final states there is a different  $c_u$  and  $c_d$ . Interestingly,  $U(1)$  gauge groups that lead to a  $Z'$  of this type exist even when the anomalies cancel without need for new fermions charged under the SM group, and the quark and lepton masses are generated by Yukawa couplings to a single Higgs-doublet. Such  $Z'$  bosons may have very small couplings to electrons, evading altogether the LEP bounds, and could be discovered in the  $\mu^+\mu^-$  or  $\tau^+\tau^-$  channels at the Tevatron.

Although generation-independent  $Z'$  couplings to quarks are tightly constrained by measurements of various flavor-changing neutral currents, a  $Z'$  with different couplings to the  $d$  and  $s$  quarks (or to the  $u$  and  $c$  quarks) in the mass range accessible at the Tevatron cannot be completely ruled out. In that case, the  $c_u$  and  $c_d$  parametrization would have to be supplemented by  $c_s$  (or  $c_c, c_b$ ) quantities. Even in this case, the fact that current- and

next-generation hadron colliders collide nucleons (and antinucleons) implies that  $c_u$  and  $c_d$  typically remain the most important, because of their large valence distribution functions (particularly at large parton  $x$ ) for nucleons.

Observables other than the total cross section for dilepton production can also be measured at the Tevatron. We have discussed the additional information provided by the forward-backward asymmetry. In most cases however, a  $Z'$  discovery is more likely to occur first as a bump in the dilepton total cross section. If that happens,  $M_{Z'}$  can be determined by the invariant mass of the lepton pair, and a curve (actually a band of experimental error bars) in the  $c_u - c_d$  plane can be derived. For each  $Z'$  model (fixed  $x$  within the one-parameter families), the curve would determine the gauge coupling. However, pinning down the model would be difficult, requiring additional observables at the Tevatron and future colliders.

## ACKNOWLEDGMENTS

The authors have benefited from discussions with Ayres Freitas and Beate Heinemann. A. D. thanks the Theory Department at Fermilab for their warm hospitality and financial support, and CONICET, Argentina, for financial support. Fermilab is operated by Universities Research Association Inc. under Contract No. DE-AC02-76CH02000 with the DOE.

## APPENDIX: INTERFERENCE TERMS

The  $Z'$  interference with the  $Z$  and the photon is taken into account by the second term in Eq. (3.1). This term can be factorized similarly to the contribution due solely to

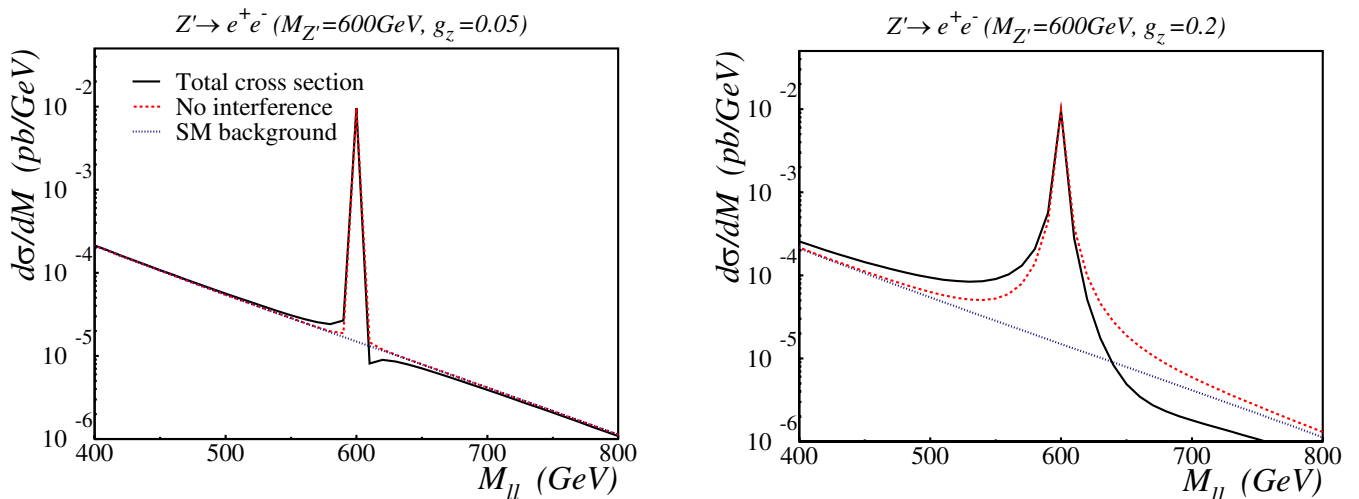


FIG. 9 (color online). NLO differential cross sections for the production of electron-positron pairs as a function of the invariant mass of the pair, in the  $U(1)_{B+L}$  model. The solid curves correspond to the total cross sections for the signal, including interference terms, for the gauge coupling fixed to  $g_z = 0.05$  and  $g_z = 0.2$  respectively. Dashed lines are the same cross sections neglecting interference terms and the dotted lines correspond to the SM background.

the  $Z'$  [first term in Eq. (3.1)], by replacing  $\sigma(Z' \rightarrow l^+l^-)$  with

$$\begin{aligned} \sigma(Z', X) &= \frac{g_z g_X}{2\pi} \left( \frac{z_{l_j} z_l^X + z_{e_j} z_e^X}{288} \right) \\ &\times \frac{(Q^2 - M_{Z'}^2)(Q^2 - M_X^2) + M_{Z'} M_X \Gamma_{Z'} \Gamma_X}{[(Q^2 - M_{Z'}^2)^2 + M_{Z'}^2 \Gamma_{Z'}^2][(Q^2 - M_X^2)^2 + M_X^2 \Gamma_X^2]}, \end{aligned}$$

where  $X = \gamma, Z^0$  and  $g_X, (z_{l_j}^X, z_{e_j}^X), M_X$  and  $\Gamma_X$  are the corresponding coupling, lepton charges and mass and width of the boson. The quark charges in  $W_{Z'}$  must also be changed accordingly in Eq. (3.1).

For a narrow  $Z'$  resonance, the interference of the  $Z'$  with the  $Z$  and photons can be neglected. As an illustration, in Fig. 9, we plot the NLO cross section for the production of an electron-positron pair as a function of the lepton system invariant mass. The curves shown correspond to the SM background for the process and to the  $Z'$  mediated ones, with and without the interference terms with the  $Z^0$  and the photon.

For the plot we chose the  $B - xL$  model, discussed in the previous section, and fixed  $M_{Z'} = 600$  GeV, and  $x = -1$ . Note that for  $x = +1$  the only difference is that the interference terms change sign. The two sets of curves correspond to different choices for the gauge coupling, namely  $g_z = 0.05$  and  $g_z = 0.2$ . These values of the coupling correspond to  $\Gamma_{Z'} = 0.26$  GeV and  $\Gamma_{Z'} = 4.15$  GeV, respectively, assuming that only decays to SM particles are allowed and neglecting all QCD and electroweak corrections. The bounds set by LEP for these two cases are  $M_{Z'} \geq 300$  1200 GeV respectively. In the case of  $g_z = 0.05$ , the signal cross section outside the  $Z'$  peak is completely negligible compared to the SM background, and, at the peak, the interference terms can be neglected. For  $g_z = 0.2$ , the interference terms are more important and contribute to the tails at low and high mass. However, the experimental errors would not allow one to disentangle the signal from the background outside the peak, where again, the signal cross section is dominated by terms containing only  $Z'$  propagators.

- 
- [1] E. Eichten, I. Hinchliffe, K. D. Lane, and C. Quigg, *Rev. Mod. Phys.* **56**, 579 (1984); **58**, 1065 (1986).
- [2] For a review, see J. L. Hewett and T. G. Rizzo, *Phys. Rep.* **183**, 193 (1989).
- [3] See, e.g., M. Cvetič and P. Langacker, *Phys. Rev. D* **54**, 3570 (1996).
- [4] For a review, see A. Leike, *Phys. Rep.* **317**, 143 (1999).
- [5] T. Appelquist, B. A. Dobrescu, and A. R. Hopper, *Phys. Rev. D* **68**, 035012 (2003).
- [6] A. Freitas, *Phys. Rev. D* **70**, 015008 (2004).
- [7] For a recent review, see, G. Altarelli and M. W. Grunewald, hep-ph/0404165 (to be published).
- [8] M. S. Chanowitz, *Phys. Rev. Lett.* **87**, 231802 (2001); *Phys. Rev. D* **66**, 073002 (2002); D. Choudhury, T. M. P. Tait, and C. E. M. Wagner, *Phys. Rev. D* **65**, 053002 (2002).
- [9] J. Erler and P. Langacker, *Phys. Rev. Lett.* **84**, 212 (2000); P. Langacker and M. Plumacher, *Phys. Rev. D* **62**, 013006 (2000).
- [10] DELPHI Collaboration, P. Abreu *et al.*, *Z. Phys. C* **65**, 603 (1995).
- [11] M. Carena, T. M. P. Tait, and C. E. M. Wagner, *Acta Phys. Pol. B* **33**, 2355 (2002).
- [12] For example, N. Arkani-Hamed, A. G. Cohen, E. Katz, and A. E. Nelson, *J. High Energy Phys.* 07 (2002) 034.
- [13] C. Csaki, J. Hubisz, G. D. Kribs, P. Meade, and J. Terning, *Phys. Rev. D* **67**, 115002 (2003); J. L. Hewett, F. J. Petriello, and T. G. Rizzo, *J. High Energy Phys.* 10 (2003) 062.
- [14] LEP Collaboration, hep-ex/0312023.
- [15] C. T. Hill, *Phys. Lett. B* **345**, 483 (1995); R. S. Chivukula and E. H. Simmons, *Phys. Rev. D* **66**, 015006 (2002).
- [16] R. S. Chivukula, E. H. Simmons, and J. Terning, *Phys. Rev. D* **53**, 5258 (1996); D. J. Muller and S. Nandi, *Phys. Lett. B* **383**, 345 (1996); E. Malkawi, T. Tait, and C. P. Yuan, *Phys. Lett. B* **385**, 304 (1996); H. J. He, T. Tait, and C. P. Yuan, *Phys. Rev. D* **62**, 011702 (2000).
- [17] P. Batra, A. Delgado, D. E. Kaplan, and T. M. P. Tait, *J. High Energy Phys.* 02 (2004) 043; 06 (2004) 032.
- [18] CDF Collaboration, F. Abe *et al.*, *Phys. Rev. Lett.* **68**, 1463 (1992).
- [19] CDF Collaboration, F. Abe *et al.*, *Phys. Rev. D* **51**, 949 (1995).
- [20] CDF Collaboration, F. Abe *et al.*, *Phys. Rev. Lett.* **79**, 2192 (1997).
- [21] D0 Collaboration, S. Abachi *et al.*, *Phys. Lett. B* **385**, 471 (1996).
- [22] D0 Collaboration, B. Abbott *et al.*, *Phys. Rev. Lett.* **82**, 4769 (1999).
- [23] D0 Collaboration, V. M. Abazov *et al.*, *Phys. Rev. Lett.* **87**, 061802 (2001).
- [24] Talk at Fermilab by Anton Anastassov, July 23, 2004, <http://theory.fnal.gov/jetp/previous.html>.
- [25] R. Hamberg, W. L. van Neerven and T. Matsuura, *Nucl. Phys.* **B359**, 343 (1991); **644**, 403(E) (2002).
- [26] D0 Collaboration, Report No. 4375-Conf (unpublished)
- [27] Tracey Pratt (for the CDF Collaboration), talk at the SUSY 2004 Conference, June 2004.
- [28] A. D. Martin, R. G. Roberts, W. J. Stirling and R. S. Thorne, *Phys. Lett. B* **531**, 216 (2002).
- [29] J. Pumplin, D. R. Stump, J. Huston, H. L. Lai, P. Nadolsky, and W. K. Tung, *J. High Energy Phys.* 07 (2002) 012.

- [30] R.V. Harlander and W.B. Kilgore, Phys. Rev. Lett. **88**, 201801 (2002).
- [31] <http://www.lorentz.leidenuniv.nl/neerven/>
- [32] U. Baur, O. Brein, W. Hollik, C. Schappacher, and D. Wackerth, Phys. Rev. D **65**, 033007 (2002).
- [33] P. Ciafaloni and D. Comelli, Phys. Lett. B **446**, 278 (1999).
- [34] U. Baur, S. Keller, and W. K. Sakumoto, Phys. Rev. D **57**, 199 (1998).
- [35] Sec. XV of MSSM Working Group Collaboration, S. Ambrosanio *et al.*, hep-ph/0006162.
- [36] Data extracted from the plots in <http://www-cdf.fnal.gov/physics/ewk/2004/afb/>